Since January 2020 Elsevier has created a COVID-19 resource centre with free information in English and Mandarin on the novel coronavirus COVID-19. The COVID-19 resource centre is hosted on Elsevier Connect, the company's public news and information website.

Bioorganic & Medicinal Chemistry 21 (2013) 3051–3057

Contents lists available at SciVerse ScienceDirect

Bioorganic & Medicinal Chemistry

journal homepage: www.elsevier.com/locate/bmc

Geranylated flavonoids displaying SARS-CoV papain-like protease inhibition from the fruits of *Paulownia tomentosa*

Jung Keun Cho [a,†], Marcus J. Curtis-Long [c,†], Kon Ho Lee [b], Dae Wook Kim [a], Hyung Won Ryu [a], Heung Joo Yuk [a], Ki Hun Park [a,*]

[a] Division of Applied Life Science (BK21 program), IALS, Gyeongsang National University, Jinju 660-701, Republic of Korea
[b] Division of Microbiology, School of Medicine, Gyeongsang National University, Jinju 660-751, Republic of Korea
[c] Graduate program in Biochemistry and Biophysics, Brandeis University, 415 South Street, Waltham, MA 02453, USA

ARTICLE INFO

Article history:
Received 17 February 2013
Revised 18 March 2013
Accepted 20 March 2013
Available online 29 March 2013

Keywords:
SARS-CoV PLpro
Paulownia tomentosa
Geranylated flavonoids
PLpro inhibitor

ABSTRACT

SARS-CoV papain-like protease (PLpro) is an important antiviral target due to its key roles in SARS virus replication. The MeOH extracts of the fruits of the *Paulownia* tree yielded many small molecules capable of targeting PLpro. Five of these compounds were new geranylated flavonoids, tomentin A, tomentin B, tomentin C, tomentin D, tomentin E (**1**–**5**). Structure analysis of new compounds (**1**–**5**) by NMR showed that they all contain a 3,4-dihydro-2*H*-pyran moiety. This chemotype is very rare and is derived from cyclization of a geranyl group with a phenol functionality. Most compounds (**1**–**12**) inhibited PLpro in a dose dependent manner with IC_{50}'s raging between 5.0 and 14.4 μM. All new compounds having the dihydro-2*H*-pyran group showed better inhibition than their parent compounds (**1** vs **11**, **2** vs **9**, **4** vs **12**, **5** vs **6**). In kinetic studies, **1**–**12** emerged to be reversible, mixed inhibitors.

1. Introduction

Between November 2002 and July 2003 world news relayed stories of a deadly disease. The disease became known as severe acute respiratory syndrome (SARS) and it is known to have caused the deaths of 916 people.[1] What is most staggering about this disease is that reported death rates were as high as 20% in the general population and can rise to over 50% in the elderly. Importantly, although no cases of SARS have been reported since 2004, the virus has not been eradicated and reservoirs of SARS-like viruses exist among bat populations.[2]

SARS is caused by the severe acute respiratory syndrome corona virus (SARS-CoV), which is a single-stranded positive-sense RNA virus that replicates in the cytoplasm of infected cells. Replication is mediated by the replicase polyprotein, which is translated directly from the viral genome, and is processed by corona viral proteases present in the replicase polyprotein. Two cysteine proteases that reside within the polyprotein, a papain-like protease (PLpro) and a 3-Chymotrypsin-like protease (3CLpro), each catalyze their own release and liberation of the other nonstructural proteins from the polyprotein. These processes are there by mandatory for virus-mediated RNA replication. PLpro serves other roles because it is not only responsible for processing the viral polyprotein but can also cleave ubiquitin chains and effect deISGylation (ISGlyation is involved in immune response to viruses).[3] Since these roles serve as virulence factors which are required for infectivity, PLpro is considered to be an attractive target for antiviral drugs.

Paulownia tomentosa steud is renowned as a polyphenol rich plant, which has been used in traditional Chinese medicine. This species belongs to the family of scrophulariaceae. Consumption of fruits of this plant is associated with a decrease in the frequency of asthmatic attacks[4] and show a hypotensive effect. An aqueous extract of fruit and leaves regenerates hair and stimulates the scalp.[5] Iridoids, lignans and flavonoids have previously been reported as bioactive compounds within *P. tomentosa*.[6] Among them, geranylated flavonoids are known as its main bioactive constituents. Some studies have reported that this species displays cytotoxic, antioxidant and antimicrobial activities.[7] Recently, geranylated flavonoid from this plant showed inhibitory activities against acetylcholinesterase and butrylcholinesterase.[8]

The aim of the present work is to investigate the PLpro inhibitory activities of *P. tomentosa* fruit extracts. We isolated a total of twelve PLpro inhibitory flavonoids of which five emerged to be new flavonoids containing a rare 3,4-dihydro-2*H*-pyran moiety. Analysis of all isolated compounds in PLpro inhibition assays showed that all species were able to inhibit the enzyme, but the novel compounds were the most effective.

Abbreviations: IC_{50}, the inhibitor concentration leading to 50 % activity loss; K_i, inhibition constant; K_m, Michaelis–Menten constant.

* Corresponding author. Tel.: +82 55 772 1965; fax: +82 55 772 1969.
E-mail address: khpark@gnu.ac.kr (K.H. Park).

† These authors equally contributed to this work.

0968-0896/$ - see front matter © 2013 Elsevier Ltd. All rights reserved.
http://dx.doi.org/10.1016/j.bmc.2013.03.027

2. Results and discussion

2.1. Structural identification of the isolated flavonoids

Starting with a methanol extract of *P. tomentosa* fruits, we purified compounds displaying PLpro inhibition by activity-guided fractionation using a SARS-CoV PLpro activity assay. Compounds (**1**–**5**) emerged to be new geranylated flavonoid derivatives which we have named tomentin A (**1**), tomentin B (**2**), tomentin C (**3**), tomentin D (**4**), and tomentin E (**5**). As shown in Figure 1, compounds (**6**–**12**) were identified as the known extracts 3′-*O*-methyldiplacol (**6**), 4′-*O*-methyldiplacol (**7**), 3′-*O*-methyldiplacone (**8**), 4′-*O*-methyldiplacone (**9**), mimulone (**10**), diplacone (**11**), and 6-geranyl-4′,5,7-trihydroxy-3′,5′-dimethoxyflavanone (**12**) by comparing our spectroscopic data (Supplementary data) and those previously reported.[6–9]

Compound **1** was isolated as a yellow oil with molecular formula $C_{25}H_{30}O_7$ established by the [M$^+$] ion at 442.1991 (Calcd 442.1992) in the HREIMS. ^{1}H and ^{13}C NMR data in conjunction with DEPT experiments indicated the presence of 25 carbon atoms, consisting of the following functional groups: 6 methylenes (sp^3), 1 methine (sp^3), 4 methines (sp^2), 3 methyls and 11 quarternary carbons (Table 1). The analysis of degrees of unsaturation indicated a tetracyclic skeleton with two aromatic rings. According to its ^{13}C and ^{1}H NMR spectra, compound **1** was found to contain an sp^3 methylene (diastereotopic protons: H_A δ_H 3.12, dd and H_B δ_H 2.74, dd) in the α-position of the carbonyl group and an oxygenated methine (δ_H 5.37 dd). The overall NMR characteristics suggested that **1** bears a flavanone backbone. The only notable feature was that H-5′ and H-6′ had the same chemical shift (δ_H 6.88) and thus were an apparent singlet (an A2 system). HMQC analysis verified that these two protons were in fact on non-equivalent carbons. The remaining proton within this ring, H-2′, was also a singlet and had a chemical shift of δ_H 7.04. The only arrangement of the ring consistent with three inequivalent proton-substituted carbons and all coupling constants 0 Hz is the proposed structure (3′,5′-disubstitution would lead to a reduction in carbon number due to symmetry and a 2′,3′-disubstitution must lead to *ortho* coupling between all three peaks). A characteristic hydrogen bonded proton signal of the C-5 (δ_C 162.7) hydroxyl group was observed at δ_H 12.47. This is consistent with C-5O*H* forming a H-bond to the isolated proton at C-8 (A ring, δ_H 6.03). The connectivity of the C ring was affirmed by COSY correlations of C-2H and C-3H2. HMBC correlation of C-2H with aromatic ring B (principally C-1′) proved the position of the B ring relative to the C ring. The presence of the stereogenic center C-2 is responsible for the chemical inequivalence of the two methylene protons at C-3. HMBC correlation of the ketone function (δ_C 197.7) with C-3H2 indicated that these two groups were juxtaposed. A weak cross peak between C-3H2 and C4a confirmed that rings A and C were fused. The presence of a 2-hydroxy-2-methylpentyl moiety was deduced from proton coupling networks across H-5″/H-6″/H-7″ in the COSY spectrum and also HMBC correlations between H-7″/C-8″, C-9″ and C-10″. The presence of two methylene functions at C-1″ and C-2″ was confirmed from both a COSY connectivity between 2H-1″, δ_H 2.65 and 2H-2″, δ_H 1.67 as well as an HMBC correlation of H-2″ with oxygenated quarternary carbon (C-3″, δ_C 73.0). Finally, the geranyl-derived side chain was unveiled to be a 2-methyl-2-(4-hydroxy-4-methylphentyl)-3,4-dihydro-2*H*-pyran moiety by HMBC correlation of C-3″ with H-2″, H-4″ and H-5″. HMBC correlation of H1″ with C-5 (δ 162.7), C-6 (δ_C 110.7) and C-7 (δ_C 165.6) affirmed the cyclization of this side chain with C-6 and C-7 (Fig. 2). The absolute stereochemistry of **1** was elucidated as *S* on the basis of CD data (a positive absorption at 328 nm and a negative absorption at 288 nm).[6] Thus, using the above obtained spectral data, compound **1** was identified as (2*S*)-2-(3,4-dihydroxyphenyl)-5-hydroxy-8-(4-hydroxy-4-methylpentyl)-8-methyl-2,3,7,8-tetrahydropyrano[3,2-*g*]chromen-4(6*H*)-one and named tomentin A.

Compound **2** was a yellow oil having molecular formula $C_{26}H_{32}O_7$ and 11 degrees of unsaturation [HREIMS (*m*/*z* 456.2151 [M$^+$], Calcd 456.2148)]. ^{1}H and ^{13}C NMR data of **2**, fully assigned through 2D NMR experiments, closely resembled those of **1** (Table 1). The difference was the appearance of a 3 proton singlet at δ_H 3.70, corresponding to methylation of one of the hydroxy groups within the pendant 3,4-dihydroxyphenyl ring (B ring). Given the broad spectral similarities between this species and compound **1**, we focus on the position of the methyl group. The strongest HMBC correlation for the arylic O*CH*$_3$ was to a quaternary carbon at 149.4 ppm (C-4′). Correlations were also observed from C-5′*H* to C-4′ and O*CH*$_3$ implying that the methoxy group is in the *para* position to the alkyl substituent. Consistent with this arrangement, C-3′ showed a strong HMBC correlation to C-2′*H* implying that the OH group was in the *meta* position to the alkyl substituent. The absolute stereochemistry of **2** was elucidated as *S* on the basis of the CD data (a positive absorption at 333 nm and a negative absorption at 294 nm).[6] Thus, based on the above obtained spectral data, compound **2** was identified as (2*S*)-5-hydroxy-2-(4-hydroxy-3-methoxyphenyl)-8-(4-hydroxy-4-methylpentyl)-8-methyl-2,3,7,8-tetrahydropyrano[3,2-*g*]chromen-4(6*H*)-one and named tomentin B.

Compound **3** a yellow oil, had the molecular formula $C_{27}H_{34}O_8$ [M$^+$] ion at 486.2257 (Calcd 486.2254) in HREIMS. Its ^{1}H and ^{13}C NMR data, parsed out using 2D NMR experiments (Table 2) also closely resembled those of **1**. However, there were two notable differences: firstly the B ring showed only two singlets at δ_H 6.79 (H-2′) and δ_H 6.94 (H-6′); there was also a new 6 proton singlet which corresponds to two methyl groups. In conjunction with the mass spectrometric data, the B ring showed characteristics of a trioxygenated arene ($R^1 = R^2 = OCH_3$;R^3 = OH). Since H-2′ and H-6′ were

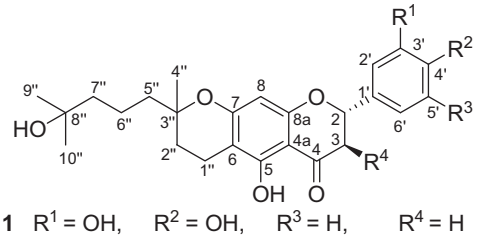

1 R^1 = OH, R^2 = OH, R^3 = H, R^4 = H
2 R^1 = OH, R^2 = OCH_3, R^3 = H, R^4 = H
3 R^1 = OCH_3, R^2 = OCH_3, R^3 = OH, R^4 = H
4 R^1 = OCH_3, R^2 = OH, R^3 = OCH_3, R^4 = H
5 R^1 = OCH_3, R^2 = OH, R^3 = H, R^4 = OH

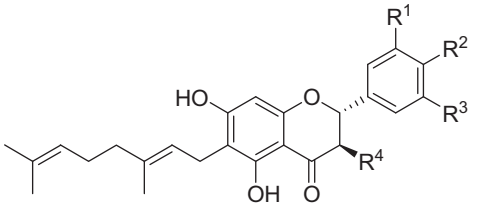

6 R^1 = OCH_3, R^2 = OH, R^3 = H, R^4 = OH
7 R^1 = OH, R^2 = OCH_3, R^3 = H, R^4 = OH
8 R^1 = OCH_3, R^2 = OH, R^3 = H, R^4 = H
9 R^1 = OH, R^2 = OCH_3, R^3 = H, R^4 = H
10 R^1 = H, R^2 = OH, R^3 = H, R^4 = H
11 R^1 = OH, R^2 = OH, R^3 = H, R^4 = H
12 R^1 = OCH_3, R^2 = OH, R^3 = OCH_3, R^4 = H

Figure 1. Chemical structures of isolated flavonoids **1**–**12** from fruits of the *Paulownia tomentosa*.

Table 1
^{1}H and ^{13}C NMR spectroscopic data (500 MHz, acetone-d_6) of compounds **1** and **2**

Position	Tomentin A (**1**)			Tomentin B (**2**)		
	δ_H (J in Hz)	δ_C	HMBC[a]	δ_H (J in Hz)	δ_C	HMBC[a]
2	5.37, dd (2.9, 12.7)	80.3	3a, 2′, 5′, 6′	5.19, dd (2.5, 12.7)	80.6	3a, 2′, 6′
3a	3.12, dd (12.7, 17.0)	44.2	2	2.97, dd (12.7, 17.1)	44.3	2
3b	2.74, dd (2.9, 17.0)			2.58, dd (3.0, 17.1)		
4		197.7	2, 3a, 3b, 8		197.7	2, 3a, 3b, 8
4a		103.5	8		115.2	2
5		162.7	1″		162.7	1″
6		110.7	8, 1″, 2″		110.7	8, 1″, 2″
7		165.6	8, 1″		165.6	8, 1″
8	6.03, s	96.0		5.88, s	95.1	
8a		162.3	2, 8		162.3	2, 8
1′		132.1	2, 3a, 2′, 6′		131.3	2, 3a, 3b, 2′, 6′
2′	7.04, s	115.2	2, 6′	6.72, s	119.6	2, 6′
3′		146.8	2′, 5′, 6′		146.7	2′, 5′
4′		146.5	2′, 5′, 6′		149.4	5′, 6′
5′	6.88, s	116.5	2′, 6′	6.57, s	103.5	2′, 6′
6′	6.88, s	119.6	2, 2′	6.57, s	108.8	2, 2′, 5′
1″	2.65, dd (4.4, 9.5)	14.7	2″	2.50, dd (5.3, 9.5)	17.7	2″
2″	1.67, dd (5.3, 9.5)	41.6	1″, 4″, 5″	1.55, dd (5.6, 9.5)	41.5	1″, 4″, 5″
3″		73.0	1″, 2″, 4″, 5″		73.5	1″, 2″, 4″, 5″
4″	1.22, s	20.0	2″, 5″	1.10, s	27.9	2″, 5″
5″	1.52, m	43.8	2″, 4″, 6″, 7″	1.39, m	43.7	2″, 4″, 6″, 7″
6″	1.46, m	17.6	5″, 7″	1.35, m	20.0	5″, 7″
7″	1.52, m	46.0	5″, 6″, 9″, 10″	1.39, m	45.9	5″, 6″, 9″, 10″
8″		70.7	6″, 7″, 9″, 10″		71.2	6″, 7″, 9″, 10″
9″	1.18, s	30.1	7″, 10″	1.05, s	30.1	7″, 10″
10″	1.18, s	30.4	7″, 9″	10.5, s	31.1	7″, 9″
4′-OCH_3				3.70, s	57.0	

[a] $^{1}H-^{13}C$ HMBC correlations are from the carbon(s) specified to the protons indicated.

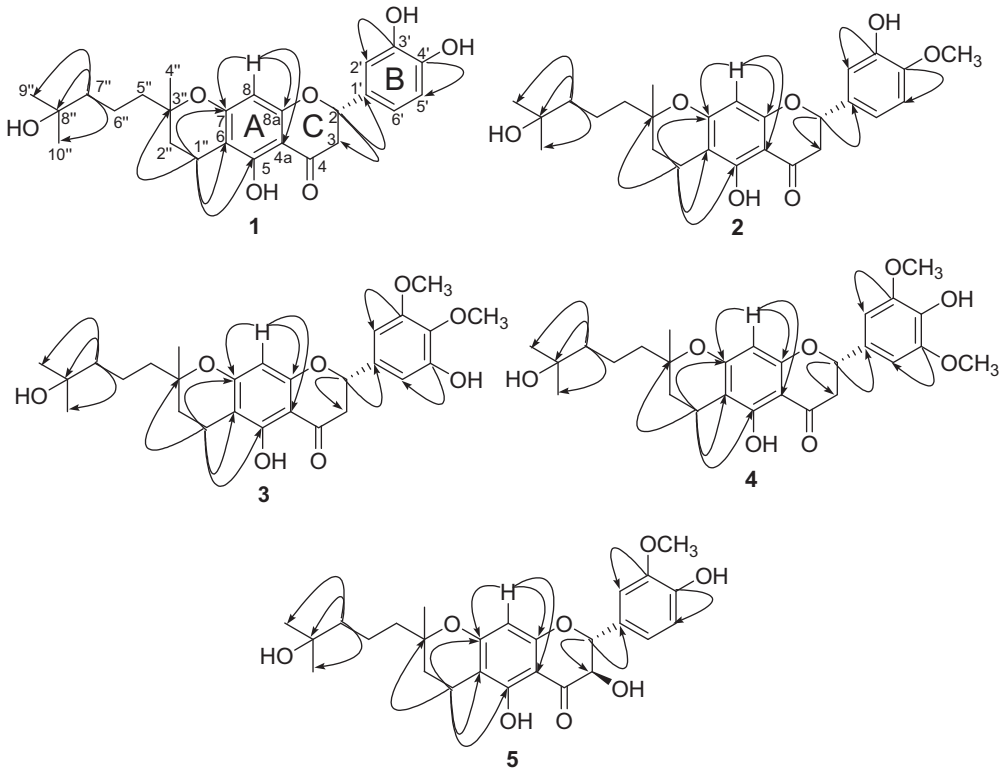

Figure 2. Selected HMBC correlations for new flavonoids **1**–**5**.

nonequivalent, the position of the lone aromatic hydroxy group must be on C-5′. The signals of δ_C 57.2 and δ_H 3.87 (6H, s) were assigned as the two methoxy groups. HMBC correlation of δ_H 3.87 with δ_C 149.2 and δ_C 146.7 further confirmed that these two *OCH₃* groups were placed on C-3′ and C-4′, respectively (Fig. 2). **3**'s absolute stereochemistry was elucidated as *S* on the basis of CD data (a positive absorption at 333 nm and a negative absorption at 296 nm).[6] Thus, compound **3** was identified as (2*S*)-5-hydroxy-

Table 2
^{1}H and ^{13}C NMR spectroscopic data (500 MHz, Acetone-d_6) of Compounds **3**–**5**

Position	Tomentin C (**3**)			Tomentin D (**4**)			Tomentin E (**5**)		
	δ_H (J in Hz)	δ_C	HMBC[a]	δ_H (J in Hz)	δ_C	HMBC[a]	δ_H (J in Hz)	δ_C	HMBC[a]
2	5.40, dd (2.8, 13.0)	80.8	3a, 2′, 6′	5.25, dd (2.9, 13.0)	80.8	3a, 2′, 6′	5.05, d (11.6)	85.1	3, 2′, 6′
3a	3.22, dd (13.0, 17.1)	44.4	2	3.06, dd (13.0, 17.1)	44.3	2	4.68, d (11.6)	73.6	2
3b	2.74, dd (2.8, 17.1)			2.59, dd (2.9, 17.1)					
4		197.7	2, 3a, 3b, 8		197.7	2, 3a, 3b, 8		198.7	2, 3, 8
4a		103.5	8		103.4	8		101.7	8
5		162.7	1″		162.7	1″		162.4	1″
6		110.8	8, 1″, 2″		110.8	8, 1″, 2″		111.1	8, 1″
7		165.6	8, 1″		165.6	8, 1″		166.2	8, 1″
8	6.06, s	96.1		5.90, s	96.1		6.03, s	96.2	
8a		162.3	2, 8		162.3	2, 8		162.1	2, 8
1′		130.9	2, 3a, 2′, 6′		130.9	2, 3a, 2′, 6′		130.2	2, 3, 2′, 5′
2′	6.79, d (1.8)	103.3	2, 6′	6.73, s	105.8	2, 6′	7.22, d (1.9)	112.8	2, 5′, 6′
3′		149.2	2′, 6′		148.9	2′, 6′		148.6	2′, 5′
4′		146.7	2′, 6′		137.7	2′, 6′		148.5	6′
5′		137.7	6′		148.9	2′, 6′	6.89, d (8.1)	115.9	2′
6′	6.94, d (1.8)	105.8	2, 2′	6.73, s	105.8	2, 2′	7.06, dd (1.9, 8.1)	122.5	2, 2′
1″	2.66, dd (4.8, 10.0)	17.7	2″	2.51, dd (5.2, 10.0)	17.7	2″	2.67, dd (4.9, 9.2)	17.7	2″
2″	1.69, dd (5.6, 10.0)	41.6	1″, 4″, 5″	1.53, dd (5.5, 10.0)	41.6	1″, 4″, 5″	1.69, dd (5.1, 9.2)	41.6	1″, 4″, 5″
3″		73.1	1″, 2″, 4″, 5″		73.1	1″, 2″, 4″, 5″		73.1	1″, 2″, 4″, 5″
4″	1.24, s	27.9	2″, 5″	1.08, s	27.9	2″, 5″	1.24, s	27.9	2″, 5″
5″	1.53, m	43.8	2″, 4″, 6″, 7″	1.37, m	43.8	2″, 4″, 6″, 7″	1.52, m	43.8	2″, 4″, 6″, 7″
6″	1.46, m	20.0	5″, 7″	1.31, m	20.0	5″, 7″	1.46, m	20.2	5″, 7″
7″	1.53, m	46.0	5″, 6″, 9″, 10″	1.37, m	46.0	5″, 6″, 9″, 10″	1.52, m	46.0	5″, 6″, 9″, 10″
8″		70.8	6″, 7″, 9″, 10″		70.7	6″, 7″, 9″, 10″		70.7	6″, 7″, 9″, 10″
9″	1.19, s	30.1	7″, 10″	1.03, s	29.8	7″, 10″	1.18, s	29.8	7″, 10″
10″	1.19, s	30.4	7″, 9″	1.03, s	30.5	7″, 9″	1.18, s	30.6	7″, 9″
3′OCH$_3$	3.87, s	57.2		3.72, s	57.2		3.89, s	56.8	
4′OCH$_3$	3.87, s	57.2							
5′OCH$_3$				3.72, s	57.2				

[a] ^{1}H–^{13}C HMBC correlations are from the carbon(s) specified to the protons indicated.

2-(5-hydroxy-3,4-dimethoxyphenyl)-8-(4-hydroxy-4-methylpentyl)-8-methyl-2,3,7,8-tetrahydropyrano[3,2-*g*]chromen-4(6*H*)-one and named tomentin C.

The yellow oil, compound **4** had the molecular formula $C_{27}H_{34}O_8$, which was established by the [M$^+$] ion at 486.2256 (Calcd 486.2254) in the HREIMS. Based upon complete assignment of the ^{1}H and ^{13}C NMR spectra of this compound using 1D and 2D techniques, closely resembled compound **3** (Table 2). However the ^{1}H NMR clearly showed a 2H singlet at δ_H 6.73. This corresponding to two arylic CHs in the B ring. Thus **4** is a regioisomer of **3** where the methoxy groups occupy the 3′ and 5′ positions on the B ring. Consistent with this symmetrical arrangement within the B ring, C-3′ and C-5′ had identical ^{13}C NMR chemical shifts at δ_C 148.9 (Fig. 2). CD analysis showed that the absolute stereochemistry of **4** was *S* (a positive absorption at 331 nm and a negative absorption at 294 nm).[6] Thus, compound **4** was identified as (2*S*)-5-hydroxy-2-(4-hydroxy-3,5-dimethoxyphenyl)-8-(4-hydroxy-4-methylpentyl)-8-methyl-2,3,7,8-tetrahydropyrano[3,2-*g*]chromen-4(6*H*)-one and named tomentin D.

Compound **5** presented as a yellow oil HREIMS delineated its molecular formula to be $C_{26}H_{32}O_8$ (*m*/*z* 472.2096 [M$^+$], Calcd. 472.2097). Thus this compound contained 11 degrees of unsaturation. ^{1}H and ^{13}C NMR data together with DEPT experiments indicated the presence of 26 carbon atoms, consisting of the following functional groups: 5 methylenes (sp^3), 2 methine (sp^3), 4 methines (sp^2), 4 methyls and 11 quarternary carbons (Table 2). The difference between this species and **1**–**4** was the appearance of one more oxygenated methine (δ_H 4.68) and disappearance of diastereotopic protons that were present in compounds **1**–**4**. The overall NMR characteristic suggested that **5** bears a dihydroflavonol backbone. The B ring was confirmed to be a 3-methoxy-4-hydroxyphenyl function as seen in compound **1**. This is clear from *ortho*-coupled protons (δ_H 6.89 for H-5′ and δ_H 7.06 for H-6′) and a singlet at δ_H 7.22 (H-2′) and HMBC correlations of C-3′ (δ_C 148.6) with *OCH*$_3$ (δ_H 3.89) (Fig. 2). The emergence of *o*-coupling (which was not observed in the compounds above) in this compound stems from the fact that H-5′ and H-6′ no longer have coincidental chemical shifts and thus are not an A2 system. The large coupling constant between H-2 and H-3 [*J* = 11.6 Hz] indicate a trans-diaxial arrangement of these two protons. This agrees with the fact that dihydroflavonols are found in nature only in the 2,3-trans configuration. The absolute stereochemistry of **5** was elucidated as 2*R*, 3*R* on the basis of CD data (a positive absorption at 332 nm and a negative absorption at 295 nm).[6] Thus, compound **5** was identified as (2*R*,3*R*)-3,5-dihydroxy-2-(4-hydroxy-3-methoxyphenyl)-8-(4-hydroxy-4-methylpentyl)-8-methyl-2,3,7,8-tetrahydropyrano[3,2-g]chromen-4(6*H*)-one and named tomentin E.

2.2. In vitro assays of SARS-CoV PLpro inhibitory activity

To investigate the relative inhibitory potency of the twelve isolated compounds (**1**–**12**) against SARS-CoV PLpro, we measured SARS-CoV PLpro activity in the presence or absence of test compounds using a fluorogenic assay. The SARS-CoV PLpro (residues 1541–1855, corresponding to the protease domain)[10] was expressed in *Escherichia coli* and purified by nickel affinity, ion-exchange and gel filtration chromatography. The apparent Michaelis constant (K_m = 52 ± 0.9 μM) was determined by plotting the initial rates normalized to enzyme concentration (52 nm) versus substrate concentration (1–104 μM), and fitting the hyperbolic data by non-linear regression using the Michaelis–Menten mode in Sigma Plot (Fig. 3A). In SARS-CoV PLpro inhibition assays, all of the compounds tested displayed dose dependent inhibition (IC_{50} 5.0–14.4 μM, Table 3). The inhibition of SARS-CoV PLpro by **2**, the most potent flavonoid (K_i = 3.5 μM), is illustrated in Fig. 3 B, C and D, representatively. Plots of residual enzyme activity versus enzyme concentration at different concentrations of compound **2** gave a family straight lines with a y axis intercept of 0; this indicates that

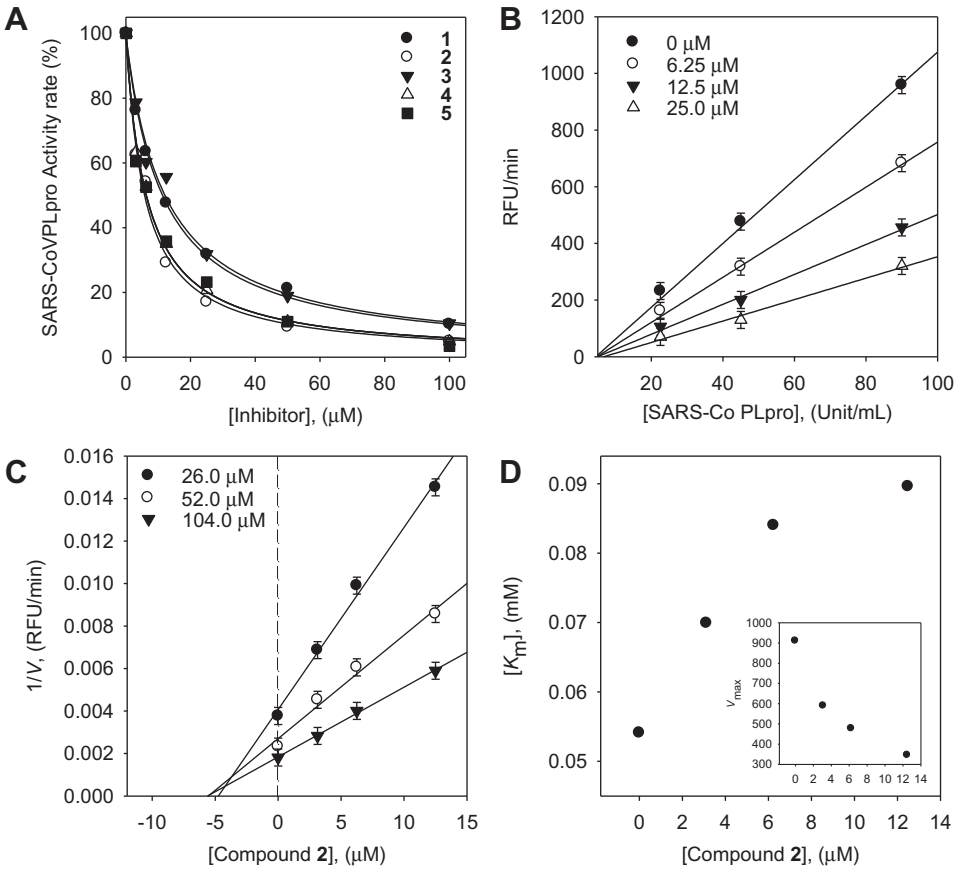

Figure 3. (A) Effects of isolated compounds **1**–**5** on the SARS-CoV PLpro catalyzed hydrolysis of Z-RLRGG-AMC. (B) The catalytic activity of SARS-CoV PLpro as a function of enzyme concentration at different concentrations of compound **2**. (C) Dixon plots of SARS-CoV PLpro inhibition by compound **2**. (D) The K_m values as a function of the concentration of compound **2**. (Inset) Dependence of the values of V_{max} on concentration of compound **2**.

Table 3
In vitro SARS-CoV PLpro inhibitory activity of compounds (**1**–**12**)

Compound	SARS-CoV PLpro (52 nM)	
	IC_{50}[a] (μM)	Kinetic mode (K_i[b], μM)
1	6.2 ± 0.04	Mixed (4.8)
2	6.1 ± 0.02	Mixed (3.5)
3	11.6 ± 0.13	Mixed (5.0)
4	12.5 ± 0.22	Mixed (13.0)
5	5.0 ± 0.06	Mixed (3.7)
6	9.5 ± 0.10	Mixed (6.6)
7	9.2 ± 0.13	Mixed (6.3)
8	13.2 ± 0.14	Mixed (7.1)
9	12.7 ± 0.19	Mixed (6.9)
10	14.4 ± 0.27	Mixed (7.8)
11	10.4 ± 0.16	Mixed (5.1)
12	13.9 ± 0.18	Mixed (8.4)

[a] All compounds were examined in a set of experiments repeated three times; error is standard deviation. IC_{50} values of compounds represent the concentration that caused 50% enzyme activity loss.
[b] Values of inhibition constant.

2 is a reversible inhibitor (Fig. 3B). The enzyme inhibition properties of target compounds were modeled using double-reciprocal plots (Lineweaver-Burk and Dixon analysis). The result show a series of lines, which intersect to the left of the vertical axis and above the horizontal axis (Fig. 3C). This implies that increasing inhibitor concentration leads to a decrease in V_{max} and an increase in K_m, indicating that compound **2** was a mixed-type inhibitor (Fig. 3D). Thus the inhibitor binds to an allosteric site on the enzyme. The K_i values of all compounds were measured by Dixon plot (Table 3).

3. Conclusion

Although SARS is most associated with the outbreaks in 2002–2003 there have been several outbreaks since this time.[11] Thus identification of new compounds with activity against essential SARS proteins is still of high importance. We set out to validate the medicinally used plant, *Paulownia tomentosa*, as a rich source of inhibitors of SARS-CoV PLpro. We chose to screen for inhibitors of this protease because it is a promising drug target since the enzyme is required for numerous processes in the viral life cycle. Our search led us to previously undisclosed natural products, which bear an unusual 3,4-dihydro-2*H*-pyran motif. This structural arrangement was found to be more effective at inhibiting SARS-CoV PLpro enzyme than the parent compounds that were cyclization precursors. This clearly underscores the importance of unearthing new or rare architectures from natural products. These novel natural products may be of general interest to the drug industry and natural product chemists.

4. Materials and methods

4.1. General experimental procedures

Circular Dichroism (CD) spectra were measured in methanol (ca 1 mg/mL) using a Jasco J-715 CD spectropolarimeter (Gross-Umstadt, Germany) and optical rotations were measured on a Perkin–Elmer 343 polarimeter. Melting points were measured on a Thomas Scientific Capillary Melting Point Apparatus and are uncorrected. NMR spectra were recorded on a Bruker AM 500

spectrometer with TMS as an internal standard, and chemical shifts are expressed in δ values. EIMS and HREIMS were obtained on a JEOL JMS-700 mass spectrometer (JEOL, Tokyo, Japan). UV spectra were measured on a Beckman DU650 spectrophotometer Infrared (IR) spectra were recorded on a Bruker IFS66 infrared Fourier transform spectrophotometer (on KBr disks). Qualitative analyses were made using a Perkin–Elmer HPLC S200 (Perkin–Elmer, Bridgeport, USA). All purifications were monitored on commercially available glass-backed Merck precoated TLC plates and visualized under UV illumination at 254 nm and/or 366 nm or stained with 10% H_2SO_4 solution. Silica gel (230–400 mesh, Merck), RP-18 (ODS-A, 12 nm, S-150 μM, YMC), and Sephadex LH-20 (Pharmacia Biotech AB, Uppsala, Sweden) were used for column chromatography. All solvents used for extraction and isolation were of analytical grade.

4.2. Plant Material

Paulownia tomentosa fruits were collected at Jinju in Gyeongsang National University, Gyeongsangnam-do, Korea, in July 2010 and identified by Prof. Jae Hong Park. A voucher specimen (KHPark 071210) of this raw material is deposited at the Herbarium of Kyungpook National University (KNU). All chemicals used were of reagent grade and were purchased from Sigma Chemical Co. (St. Louis, Mo, USA), unless otherwise stated. All solvents were distilled before use.

4.3. Extraction and Isolation

The air-dried *Paulownia tomentosa* fruits (4.0 kg) were chopped, and extracted with MeOH (10 L × 3) three times at room temperature. The combined filtrate was concentrated in vacuo to yield a dark brown gum (476 g, 11.9%). The CH_3OH extract was subjected to column chromatography (CC) on silica gel (10 × 40 cm, 230–400 mesh, 750 g) using a hexane to acetone gradient (50:1 → 1:1) to give 7 fractions (A–F). The purification of compounds **1**–**5** has not been previously reported. These five compounds together with known compounds **6**–**12** were isolated by a range of chromatographic methods. Characterization data of **6**–**12** matched with those described previously.[6–9] Fraction A (4.2 g) was fractionated by silica gel flash CC employing a gradient of hexane to acetone resulting in 9 subfractions (A1–A9). Subfractions (A3–A6, 460 mg) were purified by silica gel flash CC to yield compounds **8** (19 mg), **9** (25 mg), and **12** (18 mg). Fraction B (8.9 g) was subjected to silica gel flash CC employing a gradient of $CHCl_3$ (100%) to acetone (100%) giving 10 subfractions (B1–B10). Subfractions (B2–B8, 512 mg) were subjected to silica gel flash CC a employing hexane/acetone gradient (30:1 → 5:1) to give compounds **6** (21.6 mg), **7** (19.3 mg), and **10** (23.2 mg). Fraction C (1.8 g) was fractionated by silica gel flash CC employing a gradient of hexane (100%) to acetone (100%), resulting in 9 subfractions. Subfractions (C6–C8, 362 mg) were purified by reversed-phase CC (ODS-A, 12 nm, S-150 μM) eluting with CH_3OH/H_2O (4:1) to afford compound **11** (42 mg). Fraction D (13.1 g) was fractionated by silica gel flash CC employing a gradient of hexane (100%) to acetone (100%), resulting in 25 subfractions. Subfractions (D12–D15, 308 mg) were purified over Sephadex LH-20 (Pharmacia Biotech AB, Uppsala, Sweden) with 80% CH_3OH as eluent, yielding compounds **3** (17 mg) and **4** (13 mg). Fraction E (3.4 g) was subjected to flash CC on silica gel employing a gradient of $CHCl_3$ (100%) to acetone (100%) giving 5 subfractions (E1–E5). Subfractions (E2–E4, 472 mg) were purified by reversed-phase CC (ODS-A, 12 nm, S-150 μM) eluting with CH_3OH/H_2O (2:1) to afford compounds **1** (17 mg) and **5** (12.4 mg). Fraction F (4.6 g) was subjected to flash CC on silica gel employing a gradient of $CHCl_3$ (100 %) to EtOAc (100 %), giving 12 subfractions. Subfractions F2 and F3 were purified using Sephadex LH-20 CC, eluting with 95% CH_3OH to afford compound **2** (18 mg).

Tomentin A (1): Yellow oil; $[\alpha]_D^{25}$ −14 (*c* 0.77, MeOH); UV (MeOH) λ_{max} (log ε) 205, 292 nm; IR (KBr) V_{max} 3901, 3745, 3673, 3649, 3445, 2924, 2853, 1736, 1636, 1457 cm^{-1}; ^1H NMR and ^{13}C NMR data, see Table 1; EIMS, *m*/*z* 442 $[M]^+$; HREIMS, *m*/*z* 442.1991 (Calcd for $C_{25}H_{30}O_7$ 442.1992).

Tomentin B (2): Yellow oil; $[\alpha]_D^{25}$ −20 (*c* 0.77, MeOH); UV (MeOH) λ_{max} (log ε) 206, 293 nm; IR (KBr) V_{max} 3902, 3853, 3735, 3648, 3446, 2922, 2852, 1636, 1457, 1385 cm^{-1}; ^1H NMR and ^{13}C NMR data, see Table 1; EIMS, *m*/*z* 456 $[M]^+$; HREIMS, *m*/*z* 456.2151 (Calcd for $C_{26}H_{32}O_7$ 456.2148).

Tomentin C (3): Yellow oil; $[\alpha]_D^{25}$ −24 (*c* 0.72, MeOH); UV (MeOH) λ_{max} (log ε) 206, 294 nm; IR (KBr) V_{max} 3902, 3853, 3744, 3735, 3587, 3566, 3446, 2923, 2852, 1636, 1457 cm^{-1}; ^1H NMR and ^{13}C NMR data, see Table 2; EIMS, *m*/*z* 486 $[M]^+$; HREIMS, *m*/*z* 486.2257 (Calcd for $C_{27}H_{34}O_8$ 486.2254).

Tomentin D (4): Yellow oil; $[\alpha]_D^{25}$ −23 (*c* 0.67, MeOH); UV (MeOH) λ_{max} (log ε) 206, 294 nm; IR (KBr) V_{max} 3743, 3448, 2924, 2852, 1736, 1637, 1459, 1161, 1117 cm^{-1}; ^1H NMR and ^{13}C NMR data, see Table 2; EIMS, *m*/*z* 486 $[M]^+$; HREIMS, *m*/*z* 486.2256 (Calcd for $C_{27}H_{34}O_8$ 486.2254).

Tomentin E (5): Yellow oil; $[\alpha]_D^{25}$ −7 (*c* 0.57, MeOH); UV (MeOH) λ_{max} (log ε) 203, 218, 295 nm; IR (KBr) V_{max} 3745, 3445, 2924, 2853, 1636, 1457, 1121 cm^{-1}; ^1H NMR and ^{13}C NMR data, see Table 2; EIMS, *m*/*z* 472 $[M]^+$; HREIMS, *m*/*z* 472.2096 (Calcd for $C_{26}H_{32}O_8$ 472.2097).

4.4. Expression and purification of SARS-CoV PLpro from *E. coli*

The gene encoding the PLpro (945 bp) was amplified from the plasmid pSARS-REP (*SARS-CoV* ulbani strain, Genbank AY278741) using forward primer 5′-GCGGGATCCGAGGTTAAGACTATAAAAG TGTTC and the reverse primer 5′-GCGCTCGAGTTACTTGATGGTTGT AGTGTAAGA (*BamHI* and XhoI sites are underlined). The gene was ligated into a PCR-TOPO (Invitrogen, USA) and the inserted gene was confirmed by DNA sequencing with T7 forward and T7 terminal reverse primers. Then, the correct gene fragment was transferred into a pPRoEx HT expression vector (Invitrogen, USA) and transformed into DH5α competent cells. The expression plasmid was constructed to carry a His_6-tag followed by a TEV protease cleavage site at the N-terminus. Correct clones of the PLpro in the pPRoEX HT vector were identified and verified by PCR, restriction digestion with *BamHI* and *XhoI* and sequencing. The plasmid pPRoEx HT harbouring the PLpro gene was transformed into an *E. coli* strain BL21(DE3) (Novagen, Madison, WI, USA) for protein expression. A 10 ml aliquot of an overnight culture was seeded into 1000 ml of fresh LB (Luria-Bertani) medium containing 50 mg/ml ampicillin and cells were grown to $OD_{600\ nm}$ of 0.6 at 37 °C. The cells were cooled down in ice for 30 min and protein expression was induced for 5 h with 0.4 mM isopropyl β-D-1-thiogalactopyranoside (IPTG) at 30 °C. The cells were harvested by centrifugation at 6000 rpm for 6 min at 4 °C. The harvested cells were washed twice in phosphate-buffered saline. The cell pellet was used directly for purification or stored at −80 °C until use.

The cell pellet was suspended in binding buffer (50 mM NaH_2PO_4 pH 8.0, 500 mM NaCl, 5 mM imidazole and 5 mM β-mercaptoethanol) and cells were disrupted by sonication. After centrifugation at 15,000 rpm for 1 h, the clarified supernatant was collected, filtered (Qualitative filter paper, Advantec, Japan) and applied onto a column of Nickel Sepharose 6 Fast Flow (GE Healthcare, Sweden) beads pre-equilibrated with the binding buffer. The column was washed first with 20 column volumes of binding buffer and then with 2 column volumes of washing buffer (50 mM Tris–HCl pH 8.0, 500 mM NaCl, 30 mM imidazole). The recombinant PLpro proteins were eluted with the elution buffer

(50 mM Tris–HCl pH 8.0, 100 mM NaCl and 300 mM imidazole). The PLpro eluted from the nickel column was further purified by ion-exchange chromatography using a salt gradient with a SOURCE 15Q column (GE Healthcare, Piscataway, NJ, USA) in 50 mM Tris-HCl pH 8.5 and 2 mM DTT. The PLpro was finally purified by size exclusion chromatography with a Superdex 200 column (GE Healthcare, Piscataway, NJ, USA) in 20 mM Tris–HCl pH 8.0, 150 mM NaCl and 2 mM DTT. The fractions containing PLpro were pooled, exchanged into 20 mM Tris–HCl pH 8.0 and 10 mM DTT and concentrated to a final concentration of 10 mg/ml by ultrafiltration (Microcon YM-30, Millipore Corporation, Bedford, Massachusetts, USA). The protein purity was examined by SDS–PAGE and native-PAGE. The protein concentration was determined by Bradford method (Bradford, 1976) using bovine serum albumin as the standard. The N-terminal his-tag was removed by TEV digestion for activity assay.

4.5. SARS-CoV PLpro inhibition assay

IC_{50} values for all inhibitors were determined using a 96-well plate-based assay similar to our previously reported procedures.[12] The substrate used in the assay was the fluorogeneic peptide Z-Arg-Leu-Arg-Gly-Gly-AMC (Z-RLRGG-AMC), which was purchased from ENZO Life Sciences. The substrate contains the five C-terminal residues of human ubiquitin with a C-terminal 7-amido-4-methylcoumarin (AMC) group. Hydrolysis of the AMC-peptide bond dramatically increases the fluorescence of AMC, allowing conversion to be accurately determined. Reactions were performed in a total volume of 250 μL, which contained the following components: 20 mM Tris-buffer, pH 8.0, 10 mM DTT, 52 μM Z-RLRGG-AMC, 2% DMSO, and varying concentrations of inhibitor (0–200 μM). Reactions were initiated with the addition of PLpro to produce a final enzyme concentration of 52 nm. Reaction progress was monitored continuously on a SpectraMax M3Multi-Mode Microplate Reader ($\lambda_{excitation}$ = 360 nm; $\lambda_{emission}$ = 460 nm; gain = 40). Initial rate data were fit to the equation $vi = vo/(1 + [I]/IC_{50})$ using the enzyme kinetics module of Sigma Plot (v. 9.01 Systat Software, Inc.) where *vi* is the reaction rate in the presence of inhibitor, *vo* is the reaction rate in the absence of inhibitor, and [*I*] is the inhibitor concentration.

4.6. Statistical analysis

All measurements were made in triplicate. The results were subject to variance analysis using Sigma plot. Differences were considered significant at $p < 0.05$.

Acknowledgments

This research was supported by the Bio & Medical Technology Development Program of the National Research Foundation (NRF) funded by the government (MEST) (No. 20110002235). All students were supported by a scholarship from the BK21 program. MJCL acknowledges a Howard Hughes Medical Institute International Predoctoral Fellowship.

Supplementary data

Supplementary data associated with this article can be found, in the online version, at http://dx.doi.org/10.1016/j.bmc.2013.03.027.

References and notes

1. World Health Organization Geneva. *Summary table of SARS cases by country, 1 November 2002–7 August 2003*; Weekly Epidemiological Record, 2003, Vol 78, pp 310.
2. (a) Li, W.; Shi, Z.; Yu, M.; Ren, W.; Smith, C.; Epstein, J. H.; Wang, H.; Crameri, G.; Hu, Z.; Zhang, H.; Zhang, J.; McEachern, J.; Field, H.; Daszak, P.; Eaton, B. T.; Zhang, S.; Wang, L. F. *Science* **2005**, *310*, 676; (b) Lau, S. K.; Woo, P. C.; Li, K. S.; Huang, Y.; Tsoi, H. W.; Wong, B. H.; Wong, S. S.; Leung, S. Y.; Chan, K. H.; Yuen, K. Y. *PNAS* **2005**, *102*, 14040.
3. Lenschow, D. J.; Lai, C.; Frias-Staheli, N.; Giannakopoulos, N. V.; Lutz, A.; Wolff, T.; Osiak, A.; Levine, B.; Schmidt, R. E.; Garcıa-Sastre, A.; Leib, D. A.; Pekosz, A.; Knobeloch, K.-P.; Horak, I.; Whiting-Virgin, H. *PNAS* **2007**, *104*, 1371.
4. Zhao-Hua, Z.; Ching-Ju, C.; Xin-Yu, L.; Yao Gao, X.; **2008**. http://idrinfo.idrc.ca/archive/corpdocs/071235/index_e.html (cited 2005-03-1), Asian network for biological science and international development research centre, Chinese Academy of Forestry, Beijing.
5. (a) Asai, T.; Hara, N.; Sobayashi, S.; Kohshima, S.; Fujimoto, Y. *Phytochemistry* **2008**, *69*, 1234; (b) Karel, Š.; Petr, B.; Tereza, Š.; Eleonora, B.; Stefano, D.; Milan, Ž.; Gabbriella, I.; Josef, C. *Nat. Prod. Chem. Lett.* **2008**, *74*, 1488.
6. (a) Aleš, Z.; Jan, J.; Jakub, T.; Jan, M.; Pavel, S.; Gabriela, P.; Ana, L.; Milan, Ž. *Molecules* **2010**, *15*, 6035; (b) Karel, Š.; Lenka, G.; Radek, M.; Filip, L.; Dagmar, J.; Hana, F.; Ján, V.; Václav, S. *J. Nat. Prod.* **2007**, *70*, 1244.
7. Cho, J. K.; Ryu, B. Y.; Long, M. J. C.; Ryu, H. W.; Yuk, H. J.; Kim, D. W.; Kim, H. J.; Lee, W. S.; Park, K. H. *Bioorg. Med. Chem.* **2012**, *20*, 2595.
8. Damtoft, S.; Jensen, S. R. *Phytochemistry* **1993**, *34*, 1636.
9. Severe Acute Respiratory Syndrome (SARS), **2010**. http://www.health.gov.au/internet/main/publishing.nsf/content/health-sars-faq-index.htm. Australian Government Department of Health and Ageing.
10. Ratia, K.; Pegan, S.; Takayama, J.; Sleeman, K.; Coughlin, M.; Ealiji, S.; Chaudhuri, R.; Fu, W.; Prabhakar, B. S.; Johnson, M. E.; Baker, S. C.; Ghosh, A. K.; Mesecar, A. D. *PNAS* **2008**, *105*, 16119.
11. (a) Lindner, H. A.; Fotouhi-Ardakani, N.; Lytvyn, V.; Lachance, P.; Sulea, T.; Ménard, R. *J. Virol.* **2005**, *79*, 15199–15208; (b) Sulea, T.; Lindner, H. A.; Purisima, E. O.; Menard, R. *J. Virol.* **2005**, *79*, 4550.
12. Shental-Bechor, D.; Levy, Y. *PNAS* **2008**, *105*, 8256.

Update

Bioorganic & Medicinal Chemistry

Volume 21, Issue 22, 15 November 2013, Page 7229

DOI: https://doi.org/10.1016/j.bmc.2013.09.005

Bioorganic & Medicinal Chemistry 21 (2013) 7229

Contents lists available at ScienceDirect

Bioorganic & Medicinal Chemistry

journal homepage: www.elsevier.com/locate/bmc

Corrigendum

Corrigendum to "Geranylated flavonoids displaying SARS-CoV papain-like protease inhibition from the fruits of *Paulownia tomentosa*" [Bioorg. Med. Chem. 21 (2013) 3051–3057]

Jung Keun Cho [a,†], Marcus J. Curtis-Long [c,†], Kon Ho Lee [b], Dae Wook Kim [a], Hyung Won Ryu [a], Heung Joo Yuk [a], Ki Hun Park [a,*]

[a] Division of Applied Life Science (BK21 Program), IALS, Gyeongsang National University, Jinju 660-701, Republic of Korea
[b] Division of Microbiology, School of Medicine, Gyeongsang National University, Jinju 660-751, Republic of Korea
[c] Graduate Program in Biochemistry and Biophysics, Brandeis University, 415 South Street, Waltham, MA 02453, USA

Several references appeared incorrectly. The corrected references appear below.

5. (b) Šmejkal, K.; Babula, P.; Šlapetová,T.; Brognara, E.; DalÍAcqua, S.; Žemlička, M.; Innocenti, G.; Cvačka, *J. Planta Med.* **2008**, *74*, 1488.
6. (a) Zima, A.; Hošek, J.; Treml, J.; Muselík, J.; Suchý, P.; Pražanová, G.; Lopez, A.; Žemlička, M. *Molecules* **2010**, *15*, 6035.
6. (b) Šmejkal, K.; Grycová, L.; Marek, R.; Lemiere, F.; Jankovská, D.; Forejtníková, H.; Vančo, J.; Suchý, V. *J. Nat. Prod.* **2007**, *70*, 1244.

DOI of original article: http://dx.doi.org/10.1016/j.bmc.2013.03.027
* Corresponding author. Tel.: +82 55 772 1965; fax: +82 55 772 1969.
E-mail address: khpark@gnu.ac.kr (K.H. Park).
† These authors equally contributed to this work.

http://dx.doi.org/10.1016/j.bmc.2013.09.005